An Efficient Method for Computing Unsteady Transonic Aerodynamics of Swept Wings with Control Surfaces

D. D. Liu* and Y. F. Kao†
Arizona State University, Tempe, Arizona
and
K. Y. Fung‡
University of Arizona, Tucson, Arizona

A transonic equivalent strip (TES) method has been further developed for unsteady flow computations of arbitrary wing planforms. The TES method consists of two consecutive correction steps to a given nonlinear code such as LTRAN2, namely, the chordwise mean flow correction and the spanwise phase correction. The computation procedure requires direct pressure input from other computed or measured data. Otherwise, it does not require airfoil shape or grid generation for given planforms. To verify the computed results, four swept, tapered wings of various aspect ratios, including those with control surfaces, are selected as computational examples. Overall trends in unsteady pressures are established with those obtained by XTRAN3S codes, Isogai's full potential code, and measured data by NLR and RAE. In comparison with these methods, the TES has achieved considerable savings in computer time and reasonable accuracy, which suggests immediate industrial applications.

Introduction

CONSIDERABLE attention has been directed in recent years toward the technology development of transonic aeroelastic applications with particular emphasis on transonic flutter predictions. Based on transonic small-disturbance equations (TSDE), computational methods for unsteady transonic flow have been developed extensively both in two and three dimensions, notably the LTRAN2 (now ATRAN2)[1,2] and XTRAN3S computer codes. Various versions of XTRAN3S codes[3-5] and a number of full potential methods[6,7] are all in good progress. Recently, Guruswamy and Goorjian[3] and Borland and Sotomayer[4,8] have applied their versions of XTRAN3S code to the Northrop F-5 wing planform. Bennett et al.[9] have applied NASA Langley XTRAN3S codes for a RAE swept wing and Malone and Ruo[10] have applied the same code for LANN wing computations. Isogai and Suetsugu[6] have applied their full potential code to various planforms, including the AGARD standard RAE wing with an oscillating flap. Most of these results have shown good agreement with the measured data of NLR and RAE.

Although these methods can produce reasonably accurate results, computation efficiency and the grid generation procedures remain to be improved before these codes can be adopted for industrial applications. For flutter predictions and aeroelastic optimizations, a more efficient computer code capable of rapid computations is sought by the aerospace industries, since cost effectiveness is one of their main concerns.

Motivated by these considerations, we have set forth to develop a simple and more efficient method for unsteady, three-dimensional flow computations. Our objective is to achieve: 1) computation efficiency, 2) flexibility and ease of applications for flutter, and 3) a unified subsonic/transonic method for arbitrary planforms. Consequently, a preliminary version of the transonic equivalent strip (TES) method has been developed.[11] The results obtained for rectangular wing studies show promise for the TES formulation. Hence, it prompts further development. In this paper, the TES method is further developed so that all procedures are automated for aerodynamic computations. Thus, it can be readily adopted by the flutter prediction and the aeroelastic optimization programs. To validate the present method, a fairly comprehensive comparison with available data is given for a number of wing planforms including those with control surfaces.

Transonic Equivalent Strip (TES) Method

The use of strip concept for unsteady transonic computations was first proposed by the ONERA group.[12] A similar strip approach, but involving quasi-steady approximations, was recently implemented at NLR.[13] In both cases, however, only wing planforms of large aspect ratio were treated and possible applications of their methods to low-aspect-ratio wings did not seem to be forthcoming. By contrast, the present TES method is a more general scheme that can handle arbitrary planforms including oscillating control surfaces.

Correction Procedures

Specifically, the present method consists of the applications of two correction steps to the solution of a given two-dimensional code; it could be a nonlinear code such as LTRAN2 or it could be a time linearized one. The basic correction steps are: 1) the mean flow correction applied in the chordwise direction and 2) the phase correction in the spanwise direction (see Fig. 1 for flow chart). The first correction is fully automated by an inverse design procedure (IAF2 code) in that the local shock structure is properly recovered according to the given mean flow input provided by a selected computational method or by measured data. In this inverse problem, as solved by Fung and Chung,[14] the velocity potential obtained from integrating the pressure on the slit representing an airfoil is known up to an arbitrary constant. To determine this constant, a closure condition is imposed, e.g., the resulting slope distribution being equivalent to a closed body. This constant is being updated during the numerical iteration

Presented as Paper 85-4058 at the AIAA 3rd Applied Aerodynamics Conferences, Colorado Springs, CO, Oct. 14-16, 1985; received Dec. 18, 1985; revision received May 18, 1987.

*Associate Professor, Dept. of Mechanical and Aerospace Engineering. Member AIAA.
†Graduate Assistant, Dept. of Mechanical and Aerospace Engineering. Presently at Purdue University.
‡Associate Professor, Dept. of Aerospace and Mechanical Engineering. Member AIAA.

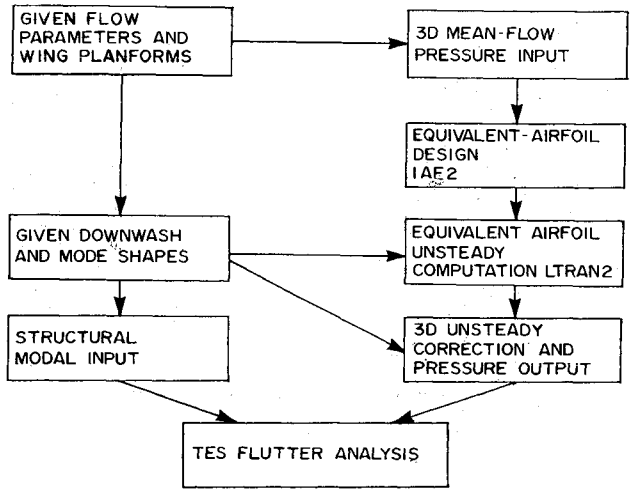

Fig. 1 Flow chart showing TES computation procedure.

process until a converged solution satisfying the closure requirement is obtained. Once the slope distribution of the new equivalent airfoil is found and the steady flowfield fixed, unsteady responses can then be calculated by varying the slopes to account for unsteady motions. The latter step can be accomplished by applying the LTRAN2 code to the equivalent airfoil.

For the second correction, we make use of the three-dimensional linear wave analogy in the sense that the phase angles are redistributed along the span according to the physical model of acoustic wave propagations in a uniform medium. This is to say that, while the first correction accounts for reproducing the nonlinear structure of the three-dimensional mean flow, the second correction is responsible for the adjustment of the spanwise phase lag of the pressure according to an equivalent linear three-dimensional flow. In practice, a typical lifting surface method such as the doublet lattice code[15] is adopted for the second correction. Clearly, shock waves cannot be created or destroyed by any process of these corrections.

We should note that the present terminology of "strip method" is defined only by the stripwise computation procedure and is otherwise irrelevant to the classical strip theory. The above correction procedures clearly indicate that the present TES approach is equivalently three-dimensional, since there is no restrictions on the wing aspect ratio.

Justification

It has been pointed out by Fung[16] and Lambourne[17], among others, that an accurate steady state with correct shock jump and location is essential for correct unsteady aerodynamic computations. It is believed that TSDE in general should be adequate for computation of unsteady disturbances, which are acoustic signals assumed to be small in conventional flutter analysis. However, when applying TSDE methods, inaccuracies may occur as a result of the local failure at the wing leading edge and the limitation in the prediction of the shock strength. Since an accurate steady-state pressure field is desired, an alternative is to find the airfoil slopes, or equivalently the airfoil, that corresponds to a given pressure distribution. This, in turn, suggests the inverse design procedure used in the first correction.

Meanwhile, the phase lag between unsteady motions of the wing and corresponding aerodynamic responses increases as the embedded supersonic region gets larger. While this effect is important in the chordwise direction of a wing, the existence of a supersonic region should not affect the way an acoustic signal propagates in the spanwise direction. With the exception of highly swept wings, the spanwise flow induced can be considered subsonic in nature. Thus, the corresponding spanwise unsteady aerodynamic responses due to small structure deformation are also subsonic and linear in nature, unlike that of the streamwise flow.

Analysis

Governing Equations

The simplest form of the time-dependent three-dimensional TSDE can be expressed as

$$C\phi_{xx} + D\phi_{yy} + \phi_{zz} = 2B\phi_{xt} + A\phi_{tt} \tag{1}$$

where

$$A = M_\infty^2 k^2/\delta^{2/3} \qquad K = (1 - M_\infty^2)/\delta^{2/3}$$

$$B = M_\infty^2 k/\delta^{2/3} \qquad \Gamma = (\gamma + 1)M_\infty^2$$

$$C = K - \Gamma\phi_x$$

$$D = c^2/b^2\delta^{2/3}$$

The nondimensional quantities and coordinates are defined as

$$\phi = \bar{\phi}/(c\delta^{2/3}U_\infty)$$

$$(x,y,z) = (\bar{x}/c,\ \bar{y}/b,\ \bar{z}\delta^{1/3}/c)$$

$$t = \bar{t}\omega \text{ and } k = \omega c/U_\infty$$

where all barred symbols denote the true physical quantities, parameters c, b, δ, and ω represent the root chord, semispan, airfoil thickness ratio, and circular frequency of oscillation, respectively.

The potential ϕ can be split into two components, i.e.,

$$\phi = \phi_0(x,z,t) + \phi_1(x,y,z,t;\Delta\alpha) \tag{2}$$

where ϕ_0 satisfies the nonlinear, two-dimensional equation [set $D = 0$ in Eq. (1)] as can be solved by the LTRAN2 code and ϕ_1 is the correction potential accounting for the three-dimensional effect attributed to a small unsteady disturbance due to the amplitude $\Delta\alpha$. The three-dimensional unsteady disturbances are assumed to be small as compared to the two-dimensional one at all times; hence, the nonlinear term in the ϕ_1 equation can be neglected, resulting in a linear equation for ϕ_1, i.e.,

$$K\phi_{1_{xx}} - \Gamma(\phi_{0_x}\phi_{1_x})_x + E\phi_{1_{yy}} + \phi_{1_{zz}} = 2B\phi_{1_{xt}} + A\phi_{1_{tt}} \tag{3}$$

The foregoing physical argument in the TES method allows for further simplification of Eq. (3) by ignoring the coupling term $(\phi_{0_x}\phi_{1_x})_x$. In so doing, Eq. (3) is reduced to the acoustic equation, where ϕ_1 can be simply solved by the conventional subsonic lifting surface method.[15]

Boundary Conditions

On the mean surface of the wing planform, the potentials must satisfy the tangency condition, i.e., at $z = 0$,

$$\phi_{0_z} = \delta F_x(x,y_i) + \alpha_0 + \alpha_1 \cdot (H_x + kH_t) \tag{4}$$

$$\phi_{1_z} = \Delta\alpha \cdot (H_x + kH_t) \tag{5}$$

where $F(x,y_i)$ is the stripwise wing surface geometry, y_i the "ith" spanwise location, α_0 the mean angle of attack, and $H(x,t)$ the wing motion with oscillation amplitude $\alpha_1 + \Delta\alpha$. While $\Delta\alpha$ is the small amplitude that induces the three-dimensional unsteady disturbances, it is actually related to the two-dimensional amplitude α_1 by $\Delta\alpha = o(\alpha_1)$.

Outside of the wing planform, the potential ϕ must satisfy

the radiation condition in the lateral and the upstream far fields. The zero-pressure-jump condition across the wake sheet and along which there is no flow discontinuity must be maintained. Also, an unsteady pressure wave must attenuate far downstream. Since these boundary conditions are linearized consistent with the small-disturbance assumption, expressions for ϕ_0 and ϕ_1 become decoupled. Thus, it renders the correction steps to be applied in a consecutive manner.

Inverse Airfoil Design (IAF2 Scheme)

At y_i, the chordwise wing surface $F(x,y_i)$ is to be replaced by an equivalent airfoil based on the inverse design method devised by Fung and Chung[14] using a given pressure distribution as input. In this scheme, the input pressure value is first integrated and the resulting potential interpolated for values at the mesh points along the airfoil slit. The airfoil closure is ascertained by rendering the integration constant vanished through the iteration procedure. The equations can then be solved on, but not necessarily, the same grid system as that of a direction calculation (AF2 scheme). Typical convergence requires 500–1000 iterations.

Pressure Coefficients

Due to a small oscillatory amplitude α, the pressure coefficient can be decomposed into

$$\bar{c}_p = c_p + \Delta c_p \cdot \alpha$$

where c_p is the steady mean pressure coefficient and Δc_p the unsteady pressure coefficient defined as

$$\Delta c_p^j = \left(\frac{P_u^j - P_l^j}{\frac{1}{2}\rho_\infty U_\infty^2} \right)' / \alpha^j \qquad (6)$$

with P_u and P_l denoting the pressure at upper and lower surfaces, superscript $j = l$, N with l denoting the linear subsonic values and N the nonlinear transonic values. Clearly,

$$\alpha^N = \alpha_1 \text{ and } \alpha^l = \Delta\alpha$$

In terms of the strip concept, Eq. (6) can be written as

$$\Delta c_{p_1}^j = c_1\, p_1^j\,(x,y,z;k) \qquad (7)$$

$$\Delta c_{p_0}^j = c_0\, p_0^j\,(x,y_i,z;k) \qquad (8)$$

where c_1 and c_0 are constants and the subscripts 0 and 1 denote, respectively, the two-dimensional strip value and the three-dimensional value at the spanwise location $y = y_i$. While the first correction is applied at the level of Eq. (6), the spanwise correction is implied by the pressure mode relation between p_1^j and p_0^j, which can be expressed as

$$p_1^j = p_0^j\, f^j(y;k) \qquad (9)$$

According to the foregoing arguments of wave propagations in the stripwise characteristic plane, the nonlinear spanwise pressure function $f^N(y;k)$ can be approximated by its linear counterpart $f^l(y;k)$ throughout the spanwise correction procedure.

In passing, we note that in all the figures presented, $\Delta c_p'$ and $\Delta c_p''$ are the real and imaginary parts of the unsteady pressure Δc_p, representing the in-phase and out-of-phase pressure coefficients.

Results and Discussion

To demonstrate the present TES method and to validate its computed results, four different wing planforms are selected for comparison with available data. These include the Northrop F-5 wing in pitching motion and with an oscillating flap, the LANN wing in pitching motion, the RAE/AGARD tailplane in pitching motion, and the AGARD standard RAE wing with an oscillating flap. The sections selected are given in Table 1. The results are shown in Figs. 2–8.

Steady Mean Flow Results: Equivalent Airfoil Design

For all steady mean flow pressure design outputs, the present computed results using the IAF2 code for equivalent airfoil design are shown by solid lines, whereas the input data in general are shown by open symbols. Figures 2a and 2b display the pressure inputs for upper and lower surfaces at the selected sections listed in Table 1 at $M_\infty = 0.82$ and 0.9 for the LANN and F-5 wings, respectively, based on the NLR's measured data.[18,19] For the case of F-5 wing at $M_\infty = 0.95$, it can be seen from Fig. 2c that "strong" shock occurs near the wing trailing edge. Hence, some care must be exercised to input the pressure data. To demonstrate the flexibility of the TES method, in Fig. 4a, we adopt the computed results of the XTRAN3S-Ames code[3] as pressure inputs. Notice that minor discrepancies between input and output results appear behind

Table 1 Selected wing sections

Planforms	Section	Semispan, %	Section	Semispan, %
F-5 wing	1	18.1	6	81.7
	2	35.2	7	87.5
	3	51.2	8	97.7
	5	72.1		
LANN wing	2	32.5	5	82.5
	3	47.5	6	95.0
	4	65.0		
RAE tailplane	1	14.0	3	66.0
	2	42.0	5	96.0

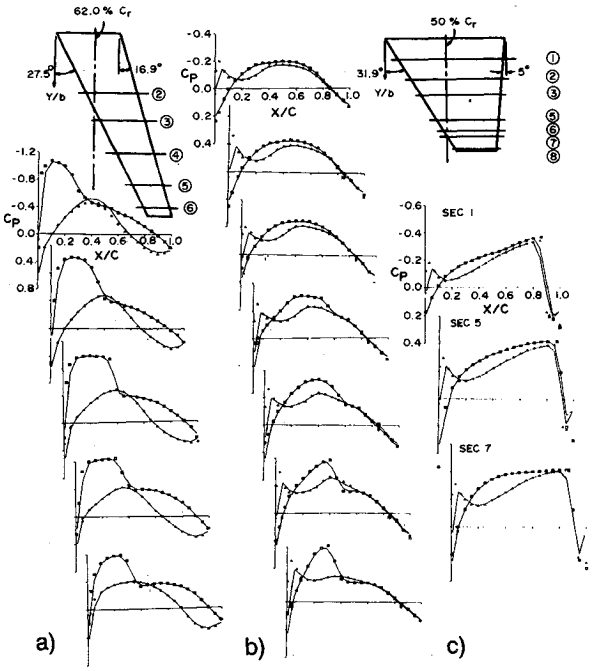

Fig. 2. Steady pressure inputs and equivalent airfoil outputs at various spanwise locations (□ upper surface, Δ lower surface, —— present TES data): a) LANN wing at mean incidence $\alpha_0 = 0.62$ deg, $M_\infty = 0.82$ (NLR measured data); b) Northrop F-5 wing at mean incidence $\alpha_0 = 0$ deg, $M_\infty = 0.90$ (NLR measured data); c) Northrop F-5 wing at mean incidence $\alpha_0 = 0$ deg, $M_\infty = 0.95$ (XTRAN3S-Ames input).

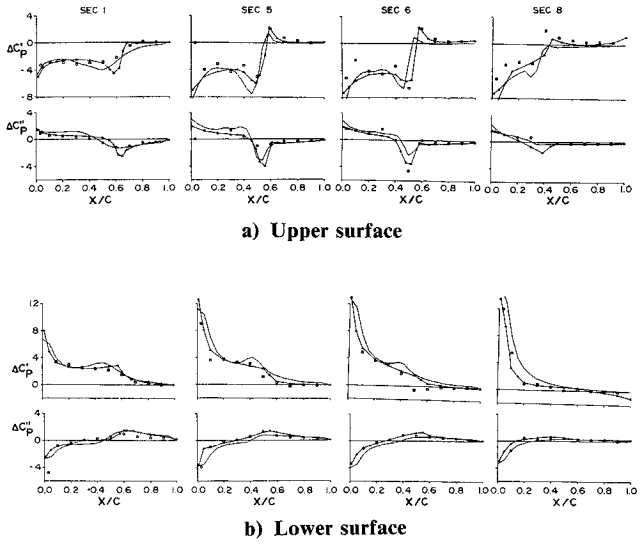

a) Upper surface

b) Lower surface

Fig. 3 Northrop F-5 wing: comparison of in- and out-of-phase pressures at four spanwise locations, pitching oscillation about midroot chord at Mach number $M_\infty = 0.90$ and reduced frequency $k_c = 0.274$ (—— present TES data, Δ XTRAN3S-Borland, □ and ○ NLR measured data).

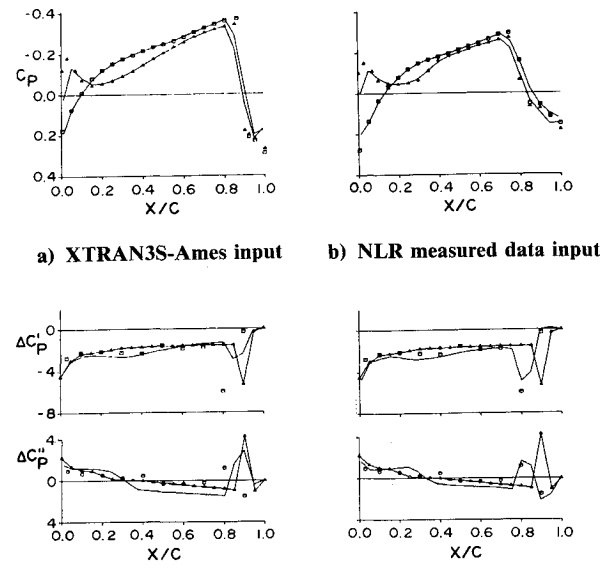

a) XTRAN3S-Ames input b) NLR measured data input

Fig. 4 Northrop F-5 wing: comparison of steady pressure distributions, in- and out-of-phase pressures at 18% spanwise locations, pitching oscillation about midroot chord at Mach number $M_\infty = 0.95$ and reduced frequency $k_c = 0.528$ (—— present TES, Δ XTRAN3S-Ames, □ and ○ NLR measured data).

the mean shock. Figure 6a shows the comparison of input data measured by RAE[9] and the TES output results for a RAE tailplane at $M_\infty = 0.9$. Figure 7 presents the steady pressures for the RAE wing at 45% spanwise location using the computed results of the Bailey-Ballhaus (or GACBOPPE) code as inputs, as no measured data were provided for this section in Ref. 20. For all cases considered, the output computed results are generally in good agreement with the input data.

Unsteady Pressure Results: LTRAN2/TES Computations

For unsteady computations, the LTRAN2 code is adopted as our computation basis because of its inclusion of nonlinearity and ease of application. In all figures presented for unsteady pressures, solid lines denote present TES method and lines attached with triangular symbols represent various versions of XTRAN3S codes, with the exception of Fig. 7. The open square and circle symbols denote the NLR or RAE measured data for in- and out-of-phase pressures, respectively.

Figure 3 contains unsteady results at various spanwise sections of the Northrop F-5 wing in pitching oscillation at $M_\infty = 0.9$ and at a given reduced frequency $k_c = 0.274$. The pitching axis of F-5 wing is located at 50% root chord. For all cases at $M_\infty = 0.9$, it can be observed that the present results practically follow the same trend as those of XTRAN3S codes. Our previous study has shown that the resulting unsteady pressures at $M_\infty = 0.95$ appear also to follow the same trend as those obtained by the NLR data and XTRAN3S code, except that the unsteady disturbances at the shock are again overpredicted by the present method. To investigate this problem further, we change the pressure input as predicted by XTRAN3S to the NLR measured data that contains a weaker mean shock. As shown in Fig. 4, the unsteady pressures are indeed improved near the shock and are otherwise unaffected. This further verifies our contention that the steady shock strength and position are the most crucial for unsteady pressure predictions.

Figure 5 presents the in- and out-of-phase pressures of the LANN wing with pitching axis located at 62% root chord. Throughout the five spanwise locations considered, the present results for upper surfaces compare more favorably with the NLR measured data than do the XTRAN3S results. Meanwhile, subcritical flows are predicted for lower surfaces; hence, the unsteady pressures do not contain shock jumps. Figure 6 presents pressure results for a highly swept RAE tailplane of $\Lambda = 50.2$ deg at $M_\infty = 0.9$ and at zero mean incidence. Because the present method uses the measured data inputs, it can be seen that the predicted unsteady shock positions correlate better with the RAE data than do the XTRAN3S results. It should be cautioned that Eq. (1) may not be suitable for wings with large sweepback angles, as the sidewash could be of the same order as the mean convective velocity. One would therefore expect that, for both steady and unsteady flows, discrepancies will occur near the wing tip, particularly for wings with low aspect ratios. Such a deterioration in pressure estimates was observed in Ref. 9.

In general, overall trends of unsteady pressures were obtained with the TES method from Figs. 3–6. In some cases, insufficient adjustment of the phase angle causes the underprediction of the unsteady pressure level. It is believed that this type of discrepancy may result from the linear approximation inherent in the spanwise correction procedure.

Oscillating Flap

Figure 7 presents the computed and measured data at 45% semispan of the AGARD standard RAE wing with an oscillating flap starting at 70% chord. It is interesting to observe that the present results and Isogai and Suetsugu's[6] full potential method are in good agreement with the RAE measured data. Figure 8 compares in- and out-of-phase pressures at two flap sections of F-5 wing at $M_\infty = 0.9$; the hinge line is located at 82% chord. Close agreements are found with XTRAN3S results of Sotomayer and Borland[8] and the NLR measured data.[21] It should be pointed out that, in presenting the flap oscillation data, the usual practice in computational methods is to connect the data points across the hinge line, in the same manner as connecting the shock points; such are the cases of Refs. 6 and 8. However, control surface singularities in subsonic flow have been well established by Landahl.[22] Since the flow is assumed inviscid and is locally subsonic, hinge line singularity, as we have presented in these figures, should prevail.

Computation Time

In performing the first correction of the present TES code (LTRAN2/IAF2), we used 103 × 97 grid points and assigned 240 time steps for each cycle. Pressure data were read in the fourth cycle, as the aerodynamic response normally became

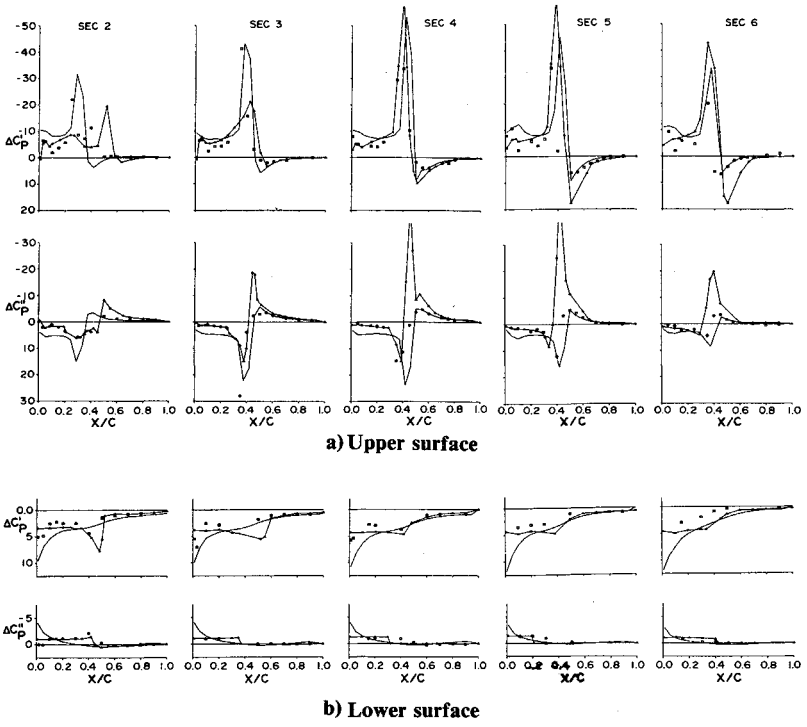

Fig. 5 LANN wing: comparison of in- and out-of-phase pressures at five spanwise locations, pitching oscillation about 62% root chord at Mach number $M_\infty = 0.82$ and reduced frequency $k_c = 0.205$ (—— present TES, Δ XTRAN3S-Malone, □ real and ○ imaginary NLR-Horsten et al. measured data).
a) Upper surface
b) Lower surface

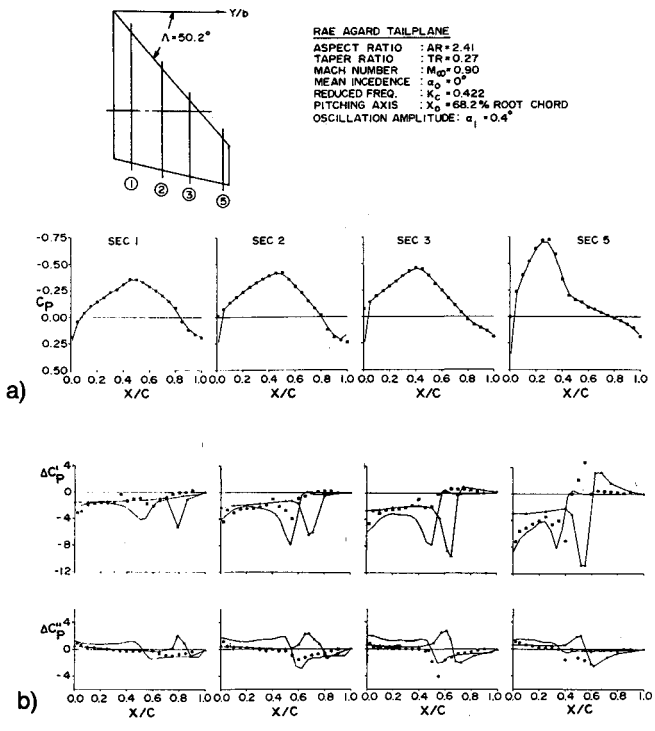

Fig. 6 RAE AGARD tailplane: comparison of pressures: a) Steady pressure inputs and equivalent airfoil pressure outputs at four spanwise locations (○ and □ RAE measured data input, —— equivalent airfoil output) b) Comparison of in- and out-of-phase pressures (—— present TES, Δ XTRANS3S-Bennet, □ and ○ RAE measured data).

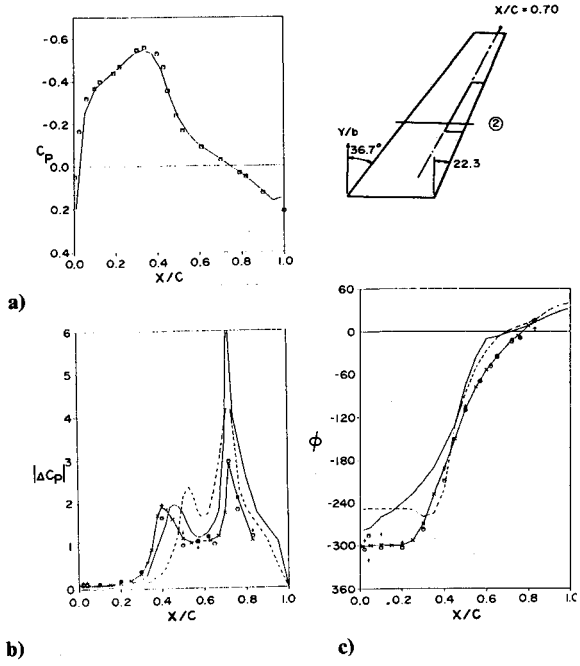

Fig 7. AGARD standard RAE wing with oscillating flap. a) Steady pressure inputs and equivalent airfoil pressure outputs at 45% spanwise location at Mach number $M_\infty =$ and mean incidence $\alpha_0 = 0$ deg (□ and ○ GACBOPPE code input, —— equivalent airfoil output) b) Pressure magnitude (—— present TES, ——, ----- Isogai's full potential, o, +, * RAE measure data) c) Phase angle on upper surface of 45% spanwise location at Mach number $M_\infty = 0.90$ and reduced frequency $k_c = 0.705$ with flap amplitude $\delta = 1$ deg (—— present TES, ----- Isogai's full potential, o, =, * RAE measured data).

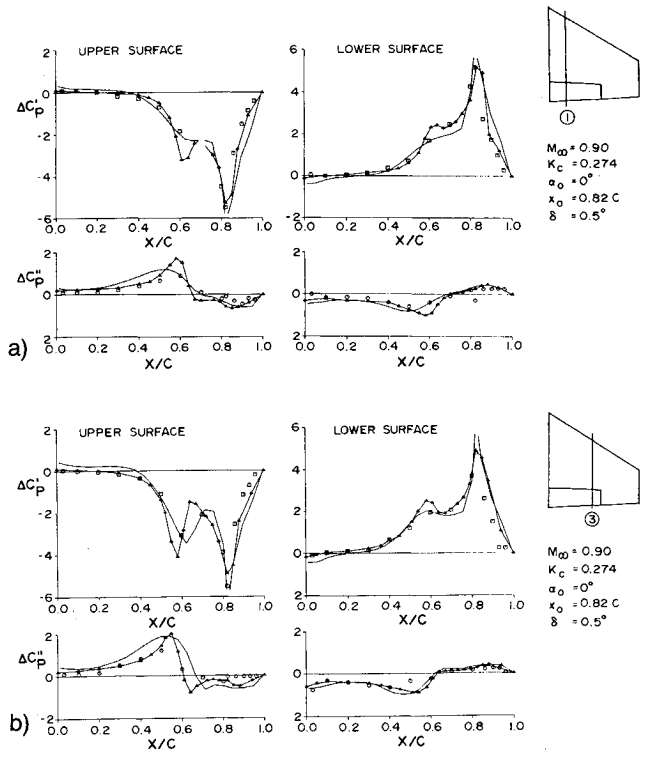

Fig. 8 Northrop F-5 wing with oscillating flap: comparision of in- and out-of-phase pressures with hinge line at 82% chord at sections 1 and 3 (—— present TES, Δ XTRANS3S-Sotomayer, □ and ○ NLR measured data): a) 18% spanwise location (section 1); b) 51% spanwise location (section 3).

periodic or harmonic after the third cycle. Typically, it took 700 iterations to achieve the IAF2 steady pressure output. In an IBM 3081, the CPU time for the first correction was some 620 s. With 10×10 panels, the doublet lattice code required 40 s; with the additional procedure, the CPU time amounted to roughly 100 s. Hence, the total CPU time required for running TES code on one strip totaled 720 s. The same case (e.g., Northrop F-5 wing) computed by XTRAN3S code would reportedly require 2000–4000 CPU time on the Cray-1S supercomputer. This would amount to an equivalent CPU time in an IBM 3081 of about 10 h or more. With the four strips chosen in this case, the present TES method usually took no more than 3000 s. Therefore, a saving of about ten- to twelvefold in CPU time can be achieved. With further improvement to the TES pilot code, it is expected that at least another reduction factor of two in CPU time can be achieved.

Conclusions

A TES method has been developed for unsteady transonic computations about wing planforms. Four swept, tapered wings of various aspect ratios including control surfaces are selected as computational examples for validation of the TES computer code. Computed results of the TES code practically follow the same trends as those of XTRAN3S codes and full potential code; all of them have been verified with available measured data by NLR and RAE.

In view of the satisfactory results obtained and the effective procedures established by the TES method, we believe that it is useful for immediate aeroelastic applications. To summarize, the following special features of the TES method are worthy of notice:

1) Applicability to general planforms. In addition to its applicability to rectangular wings, the TES method is equally applicable to swept and tapered wing planforms of any given aspect-ratio, including those with control surfaces.

2) No need for grid generation. Any time-domain, three-dimensional computational method generally requires a grid generation procedure, which can be planform dependent in most cases. The present TES method does not require such a procedure.

3) Computation efficiency. A rough estimate in CPU time indicates that to compute aerodynamics for one given mode, using the present TES code, is at least 10 times faster than using the XTRAN3S code. With further improvement of the current TES pilot code, it is expected that at least another reduction factor of two in CPU time can be achieved.

4) Flexibility and ease of application. Unlike other unsteady computational methods, the TES method makes use of the steady-flow pressures supplied either by measurement or by a steady computational method. The flexibility of the TES method lies in the pressure input scheme, which does not require airfoil shapes. For ease of application, the input format of the TES code will be unified with that of the subsonic doublet lattice code.

5) Transonic AIC and flutter. With the exclusion of chordwise bending modes, the present TES method can be extended to the construction of a three-dimensional, aerodynamic influence coefficient (AIC) matrix, hence, the generalized forces. These are the essential building blocks for the TES method to become an efficient aerodynamic tool for flutter analysis.

Acknowledgments

This work was carried out under the contract support of DTNSRDC/NAVAIR, monitored by Dr. T.C. Tai. The use of the NASA Ames Cray-1S computer for performing this research is supported under the NASA Ames/ASU Memorandum of Agreement, initiated by Drs. Peter Goorjian and Paul Kutler of the NASA Ames Applied Computational Aerodynamics Branch. The authors would like to thank Dr. P. Garcia-Fogeda of Arizona State University and Drs. G. Guruswamy and P. Goorjian of NASA Ames for valuable discussions. They also would like to thank Dr. Dale Cooley of AFWAL for supplying the LANN wing data and Mr. W. Sotomayer of AFWAL and Dr. Song Ruo of Lockheed-Georgia Co. for providing their computed results using XTRAN3S codes.

References

[1]Ballhaus, W.F. and Goorjian, P.M., "Implicit Finite-Difference Computations of Unsteady Transonic Flows about Airfoils," *AIAA Journal,* Vol. 15, Dec. 1977, pp. 1728–1735.

[2]Ballhaus, W.F. and Goorjian, P.M., "Computation of Unsteady Transonic Flows by the Indicial Method," *AIAA Journal,* Vol. 16, Feb. 1978, pp. 117–124.

[3]Guruswamy, P. and Goorjian, P.M., "An Efficient Coordinate Transformation Technique for Unsteady Transonic Aerodynamic Analysis of Low-Aspect-Ratio Wings," AIAA Paper 84-0872, 1984.

[4]Borland, C.J. and Sotomayer, W.A., "An Algorithm for Unsteady Transonic Flow about Tapered Wings," AIAA Paper 84-1567, 1984.

[5]Edwards, C.J., Bland, S.R., and Seidel, D.A., "Experience with Transonic Unsteady Aerodynamic Calculations," NASA TM 86278, Aug. 1984.

[6]Isogai, K. and Suetsugu, K., "Numerical Calculations of Unsteady Transonic Potential Flow Over Three-Dimensional Wings with Oscillating Control Surfaces," *AIAA Journal,* Vol. 22, April 1984, pp. 478–485.

[7]Malone, J.B. and Ruo, S.Y., "Computation of Unsteady Transonic Flows about Two-Dimensional and Three-Dimensional AGARD Standard Configurations," Paper presented at AGARD Specialist Meeting on Transonic Unsteady Aerodynamics and Its Aeroelastic Applications, Toulouse, France, Sept. 1984.

[8]Sotomayer, W.A. and Borland, C.J., "Numerical Computation of Unsteady Transonic Flow about Wings and Flaps," AIAA Paper 85-1712, 1985.

[9]Bennett, R.M., Wynne, E.C., and Mabey, D.G., "Calculations of Transonic Steady and Oscillatory Pressures on a Low Aspect Ratio Model and Comparison with Experiment," Paper 85-17 presented at

2nd International Symposium on Aeroelasticity and Structural Dynamics, Aachen, FRG, April 1985.

[10]Malone, J.B. and Ruo, S.Y., "LANN Wing Test Program: Acquisition and Application of Unsteady Transonic Data for Evaluation of Three-Dimensional Computational Methods," AFWAL-TR-83-3006, Feb. 1983.

[11]Liu, D.D., "Computational Transonic Equivalent Strip Method for Applications to Unsteady 3D Aerodynamics," AIAA Paper 83-0261, 1983.

[12]Couston, M., Angelini, J.J., and Meurzec, J.P., " Comparison des Champs de Pression Instationnaire Calcules et Mesure sur le Modele ZKP," AGARD-R-688, April 1980, pp. 1-1 – 1-16.

[13]Zwann, R.J., "Verifications of Calculation Methods for Unsteady Airloads in the Prediction of Transonic Flutter," AIAA Paper 84-0871, 1984.

[14]Fung, K.Y. and Chung, A., "Computations of Unsteady Transonic Aerodynamics Using Prescribed Steady Pressures," *Journal of Aircraft,* Vol. 20, Dec. 1983, pp. 1058-1061.

[15]Rodden, W.P., Giesing, J.P., and Kalman, T.P., "New Developments and Applications of the Subsonic Doublet Lattice Method for Nonplanar Configurations," Paper 4 presented at AGARD Symposium on Unsteady Aerodynamics for Aeroelastic Analyses of Interfering Surfaces, May 1970.

[16]Fung, K.Y., "A Simple, Accurate and Efficient Algorithm for Unsteady Transonic Flow," *Recent Advances in Numerical Methods in Fluid Dynamics,* edited by W.G. Habashi, Pineridge Press, Swansea, UK, 1984.

[17]Lambourne, N.C., "Experimental Techniques in Unsteady Aerodynamics," *Special Course on Unsteady Aerodynamics,* AGARD Rept. 679, June 18, 1980, pp. 10-1 – 10-26.

[18]Horsten, J.J., Den Boer, R.G., and Zwaan, R.J., "Unsteady Transonic Pressure Measurements on a Semi-Span Wing Tunnel Model of a Transport-Type Supercritical Wing (LANN Model)," NLR TR-82-069U, Pts. I and II and AFWAL-TR-83-3039, Pts. I and II, March 1983.

[19]Tijdeman et al., "Transonic Wing Tunnel Tests on an Oscillating Wing Using External Store, Part II: The Clean Wing," NLR TR 78106U, Pt. II and AFFDL-TR-78-194, Jan. 1978.

[20]Mabey, D.G., McOwat, D.M., and Welsh, B.L., "Aerodynamic Characteristics of Moving Trailing-Edge Control at Subsonic and Transonic Speeds," *Aerodynamic Characteristics of Controls,* AGARD CP-262, May 1982, pp. 20-1 – 20-25.

[21]Persoon, A.J., Roos, R., and Schippers, P., "Transonic and Low Supersonic Wind-Tunnel Tests on a Wing with Inboard Control Surface," AFWAL-TR-80-3146, Dec. 1980.

[22]Landahl, M.T., "Pressure-loading Function for Oscillating Wings with Control Surfaces," *AIAA Journal,* Vol. 6, March 1968, pp. 345-348.